サブテーマ名
小型高輝度X線発生装置を用いた X線位相イメージング法の開発

東北大学　多元物質科学研究所
百生　敦
Margie P. Olbinado

Grating Parameters

Grating Type	Source Grating, G0	Phase Grating, G1 π/2 phase shift at 30 keV	Analyzer Grating, G2
Material	Au	Ni	Au
Period (μm)	6.82	3.57	7.49
Structure Height (μm)	Design: 70 Measured: >70 +-10%	Design: 5.23 Measured: 5.34 +- 0.35	Design: 100 Measured: 103
Grating on 4-inch Si wafer	50 x 50 mm^2 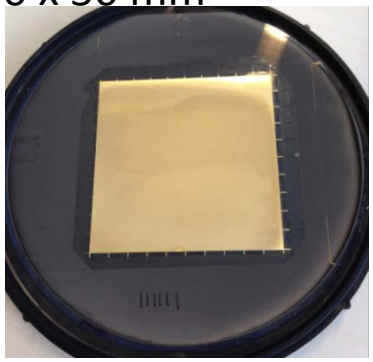	50 x 50 mm^2 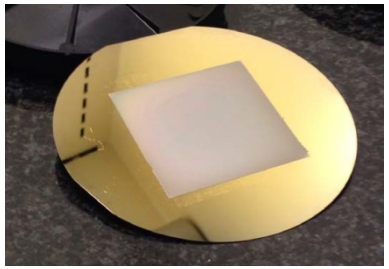	Diameter: 70mm 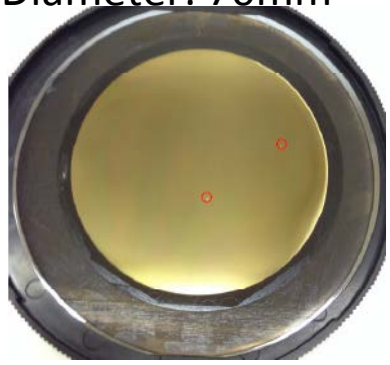
Structures	H 10 μm 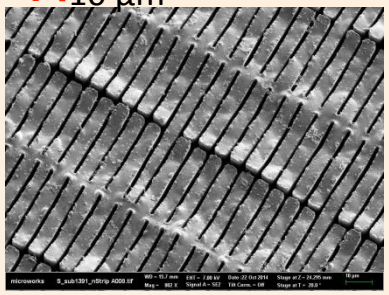 SEM	H 1 μm 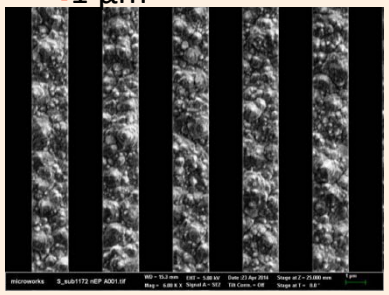 SEM	H 10 μm 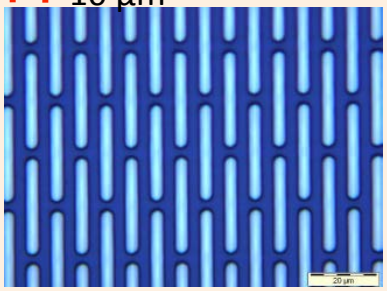

- Evaluation of the gratings' performance in X-ray Talbot-Lau interferometry was performed by measuring the Moiré fringe visibility via fringe scanning. G2 was moved across one period d2 in steps of d2/5.

- The visibility was calculated from images captured by (1) an area detector and (2) an energy-resolving detector.

X-ray Talbot-Lau Interferometer

X-ray Source	Hamamatsu Photonics Micro-focus Source (Large focus mode) Source size: 300 µm Tube Voltage: 50 kV Tube Current: 300 µA
X-ray Detector	Area Detector: 40 µm GOS scintillator connected to CCD Camera via fiber coupling (Spectral Instruments) Pixel size: 18 µm Sensor Size: 3800 x 3800 pixels^2 (68.4 x 68.4 mm^2) Energy-resolving Detector: AMPTEK CdTe diode Pinhole: 1mm, Pinhole thickness: 1mm W
Design Energy	30 keV

XTLI Set-up

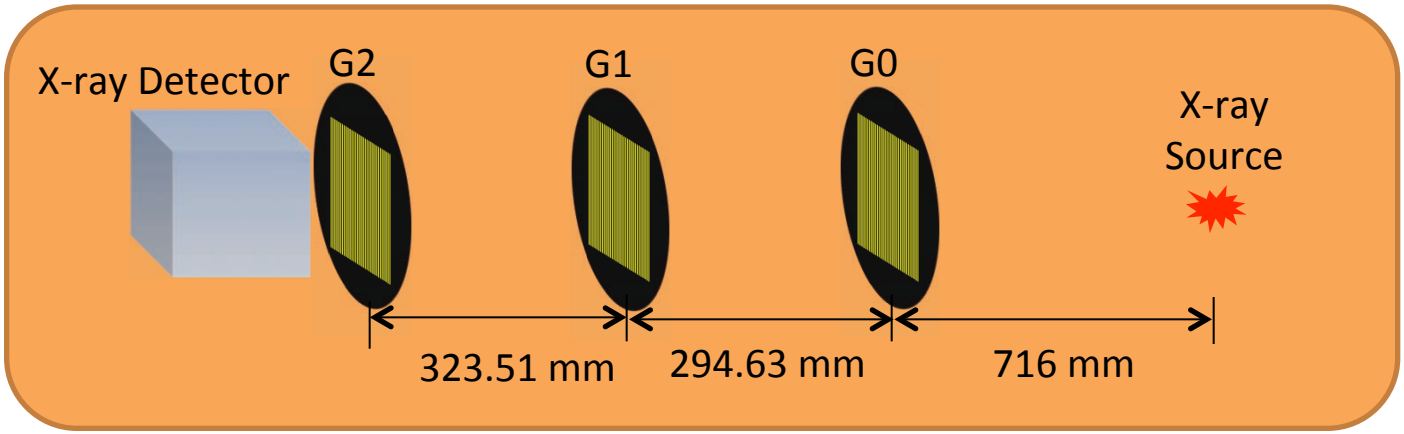

Results using the area detector

Moiré Image (Exposure time: 60 seconds)

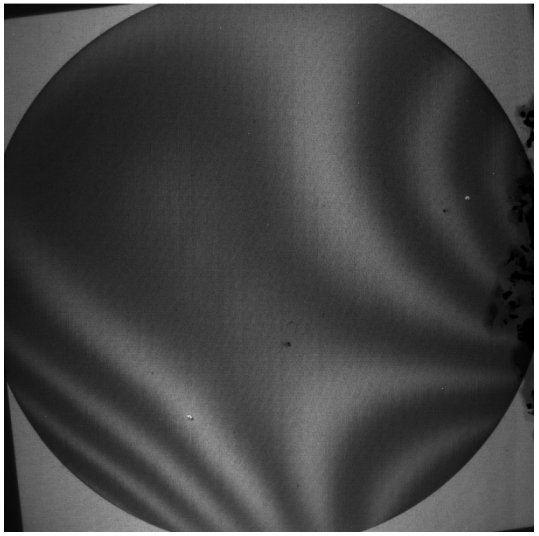

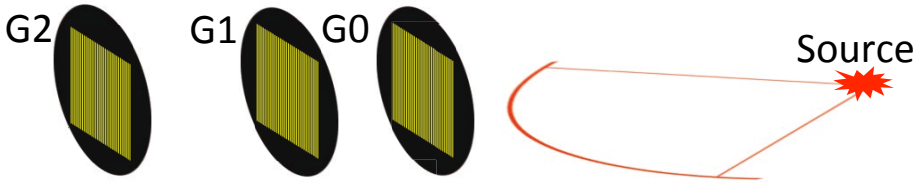

Moiré Visibility Map via 5-step fringe scan

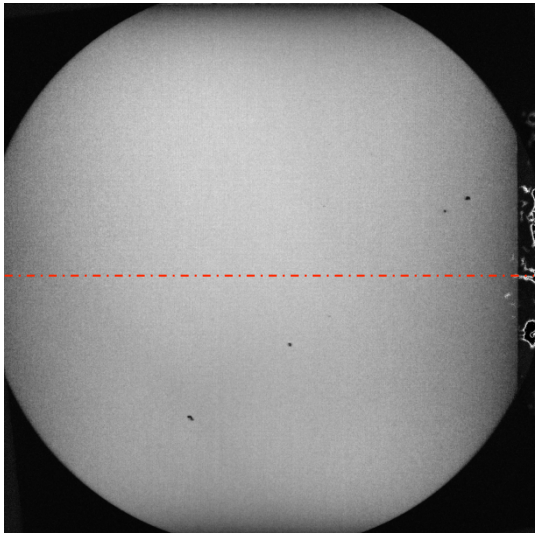

The maximum fringe visibility was 38%.

The visibility decreases away from the center of the grating. This may be a consequence of beam hardening at the sides due to cone beam illumination.

Horizontal line profile

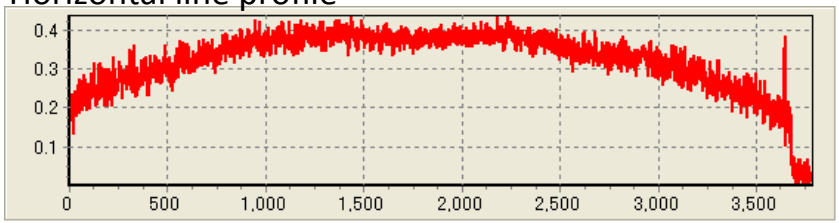

Results using the energy-resolving detector

Moiré Fringe Visibility vs. X-ray energy via 5-step fringe scan (Accumulation time per step: 10 minutes)

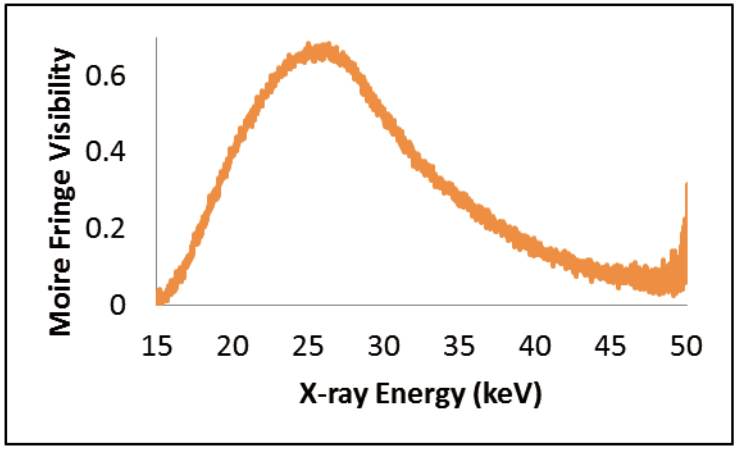

The maximum visibility can be observed at 25 keV.
This is an indication that the phase grating height corresponds to a π/2 phase shift at 25 keV. The height of Nickel was different from the designed value.

The manufacturer confirmed that height of Nickel could be less than the specified value; but they do not have an exact/ direct measurement of the grating structure height.

Comparison with the 3-grating set used with X-LCS experiment

The performance of the interferometer (SET 1) is compared with another 3-grating set (SET 2) that was previously used with the LCS X-ray Source at a design energy of 25 keV. The parameters are as shown:

Grating Parameters	SET 1	SET 2
G0 period, d0 (μm)	6.82	22.7
G0 duty cycle	0.26	0.35
G0 height (μm)	70	65
G1 period, d1 (μm)	3.57	4.36
G2 period, d2 (μm)	7.49	5.4
G2 height (μm)	100	70

Grating distances at 25 keV	SET 1	SET 2
Source- G0 (mm)	706	706
G0 – G1, R1 (mm)	245.5	995
G1 – G2, z (mm)	269.6	237.6
Source – G2, R2 (mm)	1221.1	1938.6

- **SET 1**
  - **Smaller G0 duty cycle, Higher G2 structure height → better visibility**
  - **Shorter interferometer length R2 → more (cone-beam) X-rays are detected**

Higher visibility + higher X-ray intensity = better sensitivity to X-ray phase imaging

Comparison with the 3-grating set used with X-LCS experiment

The figures on the right shows sum of 5 moiré images during fringe scan for (a) grating SET 1 and (b) SET 2. The profiles of the total intensity (normalized), moiré fringe visibility and standard deviation of the differential phase image at the indicated blue (SET 1) and red (SET 2) lines are shown below.

SET 1

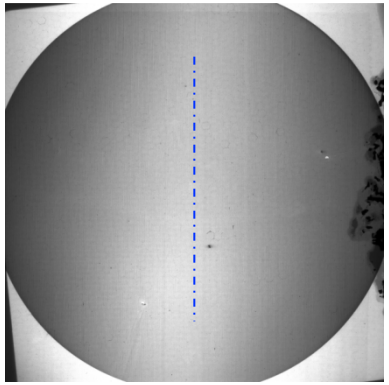

SET 2

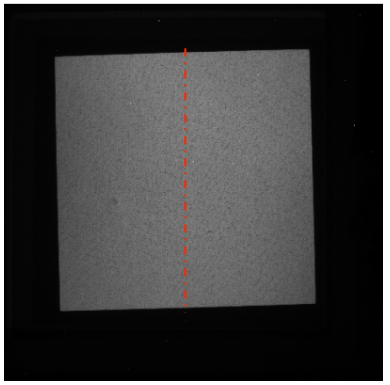

Normalized Total Intensity, I

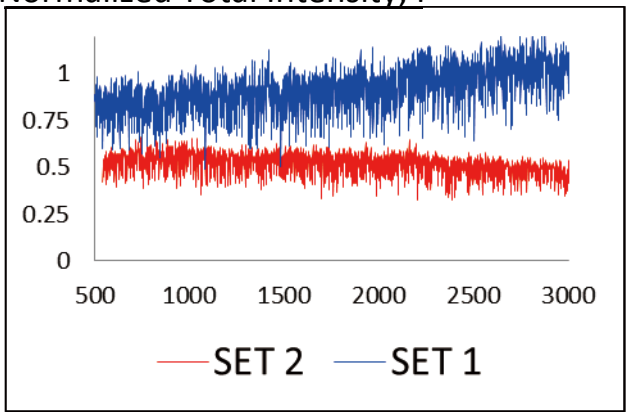

Moiré Fringe Visibility, V

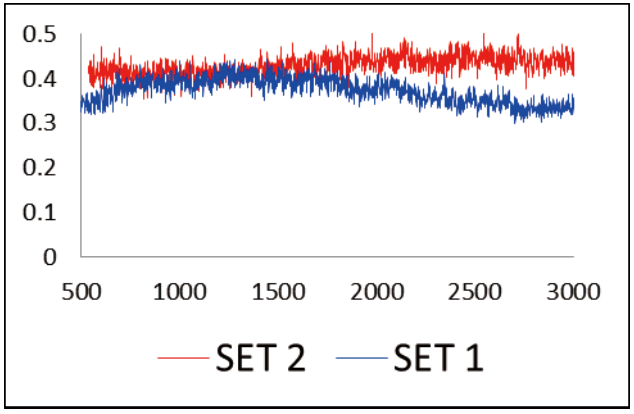

Standard Deviation of Differential Phase

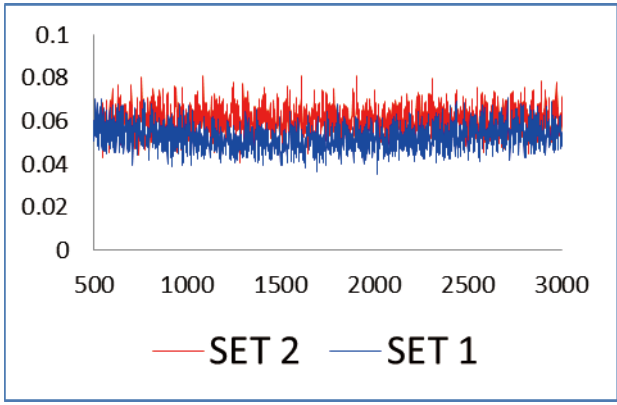

$I_{SET\ 1} > I_{SET\ 2}$
$V_{SET\ 1} < V_{SET\ 2}$
As a result, phase sensitivity for SET 1 and SET 2 is almost the same. (The sensitivity is proportional to the standard deviation of the differential phase image.)

Discussion

Although the G0 duty cycle is smaller and the grating heights of G0 and G2 are higher for SET 1, the observed visibility was lower. This is attributed to the use of bridge structure in the absorption gratings G0 and G2 as shown in the images below. In contrast, SET 2 uses continuous lamellas for G0 and sunray structure for G2.

SET 1, G0

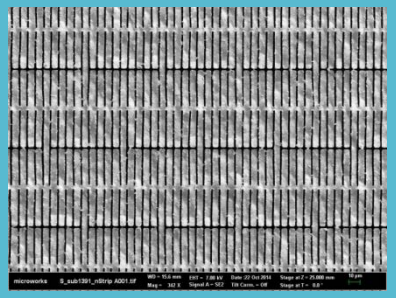

SET 1, G2

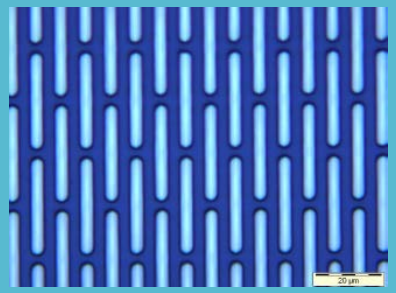

SET 2, G0

SET 2, G2

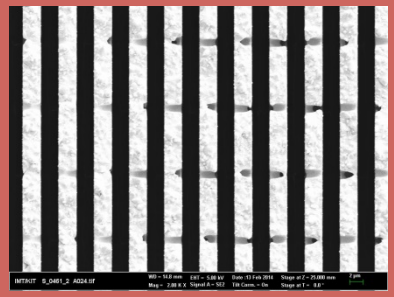

Although more X-rays are detected for SET 1, the lower visibility resulted to a phase imaging sensitivity that is almost similar with SET 2.

Summary and Conclusion

The set of gratings composed of a source grating, a π/2 phase grating and an analyzer grating for X-ray Talbot-Lau interferometry has been evaluated. Using a ccd-based X-ray detector, the maximum fringe visibility was 38%. Using an energy-resolving detector, the maximum fringe visibility was observed at 25 keV. The grating set is therefor optimum for a design energy of 25 keV. The visibility is lower but the sensitivity to X-ray phase imaging is almost similar with the grating set used in X-ray Talbot-Lau interferometry with the LCS X-ray source. The lower visibility is attributed to the bridge structures on the source grating and the analyzer grating.